Development and Testing of Femtosecond Laser Surface Processing (FLSP) Treated Guide Vanes for Application to Advanced Cryogenic Liquid Acquisition Devices

Craig Zuhlke[1], Garrett Beard[2]
University of Nebraska-Lincoln, Lincoln, NE, 68506

Tom Conboy[3]
Creare, Hanover, New Hampshire 03755

Arthur Werkheiser[4]
NASA Marshall Space Flight Center, Huntsville, Al, 35812

Jason Hartwig[5]
NASA Glenn Research Center, Cleveland, OH, 44135

Liquid Acquisition Devices (LADs) are used inside propellant tanks in microgravity to collect liquid propellant to move towards the sump or outlet of a tank during expulsion or transfer. In microgravity, vehicle thrusters can produce necessary phase separation, but in the absence of thrust, surface tension is the driver of fluid behavior. Liquid in microgravity will tend to form a sphere to minimize surface area. If a LAD can be made more "attractive" to a propellant (omniphilic), then it should perform its function more effectively. This paper presents preliminary results on using femtosecond laser surface processing (FLSP) to change the wetting properties of a vane LAD. FLSP can make metals superhydrophilic or omniphilic; by controlling the applied laser parameters, the resulting micro and nanoscale surface features can be tailored to control and optimize hydrophilic/omniphilic properties. Two LAD galleries with guide vanes were recently fabricated, a control sample and an FLSP-treated sample. The LADs were ground tested and also implemented in a parabolic flight experiment. Based on contact angle and roll-off angle measurements of the surface-treated vane, FLSP appears to be a promising technique to improve efficiency of LADs.

I. Introduction

Once a spacecraft has been boosted through Earth's atmosphere and has achieved its target velocity in orbit or has even been propelled beyond Earth's "gravity well", the need to make additional propulsive maneuvers may likely require the use of liquid propellants in a reduced or microgravity environment. It is well known that gravity affects many processes in space, such as the separation of the liquid and vapor phases within a propellant tank. In general, the lowest achievable potential energy state within a tank governs the location of the liquid/vapor interface. In the standard gravity field of Earth, fluid density dictates this location because the heavier liquid settles to the bottom and the lighter vapor rises to the top. In the microgravity conditions of space however, surface tension becomes the

[1]Research Associate Professor, Electrical and Computer Engineering, University of Nebraska-Lincoln, 419 Nebraska Hall, 900 N. 16th Street, Lincoln, NE 68588-0511
[2]Graduate Student, Electrical and Computer Engineering, University of Nebraska-Lincoln, 419 Nebraska Hall, 900 N. 16th Street, Lincoln, NE 68588-0511
[3]Research Engineer, Creare, 16 Great Hollow Rd, Hanover, NH 03755
[4]Deputy Branch Chief Advanced Concepts Office, Martin Rd SW, Huntsville, AL 35808
[5]Research Aerospace Engineer, Fluids and Cryogenics Branch, 21000 Brookpark Road, Cleveland, OH, 44135, AIAA Associate Fellow

controlling mechanism for the phase separation because the liquid tends to wet the walls, leaving a gaseous core in the center. To meet vapor-free transfer requirements for both in-space cryogenic engines and cryogenic fuel depots, any one of a number of propellant management devices (PMDs) may be required inside the tank to ensure the tank outlet is sufficiently covered in liquid despite the variable gravitational and thermal conditions during a mission. When supplying cryogenic liquids to the outlet of the tank, low gravity fluid control acquisition is further complicated over storable liquid due to the low surface tension and high susceptibility to parasitic heat leak associated with cryogenic propellants. The most commonly used PMDs are vanes, sponges, and screen channel LADs [1].

A. Screen Channel Liquid Acquisition Devices

Screen channel LADs rely on capillary flow and surface tension forces for acquiring and maintaining single phase flow to the transfer line. As shown in Figure 1, these devices follow the contour of the tank wall from end to end so that there is communication between liquid and screen in any tank orientation in any gravitational environment. The channels connect to a common outlet to withdraw liquid from the tank. The channel side that faces the tank has openings covered with a tightly woven mesh screen with micron sized pores while the sides and back of the channel are solid metal. As the tank is drained, liquid is wicked across the screen and prevents the pores from drying out when coming in contact with vapor. The screen also acts as a barrier to vapor ingestion due to surface tension forces of the liquid trapped within the pores.

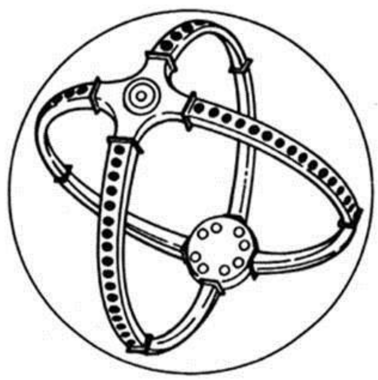

Figure 1 – Full Communication Screen Channel Liquid Acquisition Device

Screen channel LADs may be the most robust and flexible cryogenic PMD for multi-direction, multi-gravitational, multi-flow rate demand missions, which include continuous operation and restart of the engine and fluid transfer for the proposed fuel depots. For flight systems, screen channel LADs can be used as start baskets or traps to confine liquid to start engines under heavy acceleration and flow demands. Full communication screen channel LADs or tank liners as shown in Figure 1 can also be used to gather liquid in systems that experience small accelerations and small flow rate demands.

A representative LAD channel is shown in Figure 2. The channel is made of three impermeable walls with the fourth wall made of porous screen (although later designs have utilized channels with one impermeable wall and three porous walls, see [2]). The purpose of the screen is to allow liquid to flow into the channel and down to the tank outlet, and also to block vapor admittance into the channel. The screen is able to block vapor because of the capillary pressure that exists within the wetted pores of the screen. Liquid crosses the screen and is routed down the channel to the tank outlet. In an unsettled environment in microgravity, where the location of the liquid/vapor interface may be unknown, a passive LAD is the easiest and most robust and reliable method to remove vapor-free liquid from a propellant tank in both in-space engine and depot applications.

The choice of screen for a particular mission is based on many factors [3]. Screens are characterized by the weave, which describes the pattern used during manufacturing, and the coarseness or fineness of the mesh. Figure 3 shows an image of a Dutch Twill screen where each shute wire passes under one warp wire before travelling over the next warp wire. This wire pattern creates a tortuous flow path. Dutch Twills are favorable over square or twill meshes due to smaller pore sizes and the tortuous flow path created by the mesh. Fine meshes are popular candidates to counteract the effects of low surface tension cryogenic liquids, but they may generate large flow-through-screen pressure losses or become clogged by particulate matter.

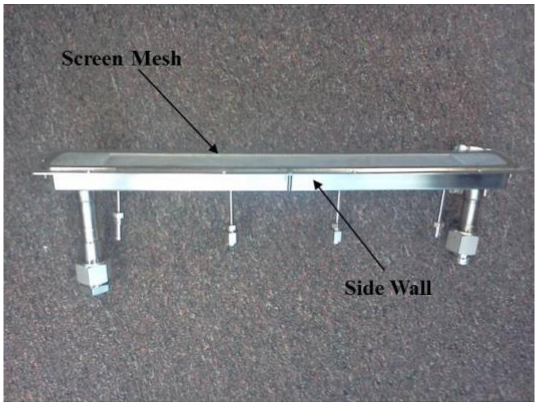

Figure 2 – Standard Laboratory Screen Channel Liquid Acquisition Device

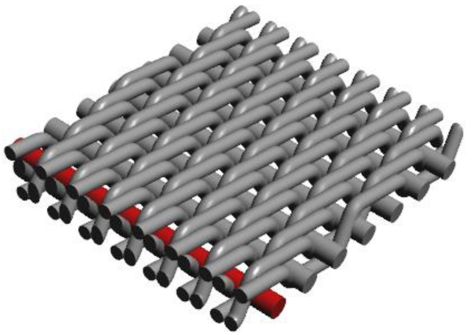

Figure 3 – 3D Image of a Dutch Twill Screen

B. Vanes

Meanwhile, as shown in Figure 4, vanes are generally designed as thin metal plates that are mounted perpendicular to the tank walls so that distinct corners are formed between PMD and the wall [4, 5]. The metal plates can be tapered from "short" to "tall" from the center of the tank to the tank outlet as shown. This tapering allows the vane to utilize a weak capillary pumping force to move liquid from the center or aft end to the tank outlet in the absence of gravity. The size and number of vanes is determined by the flow rate requirements and expulsion efficiency.

Figure 4 – Total Communication Vane Propellant Management Device

Vanes are sized and numbered so that there is always communication between the vane and propellant pool. Vanes can be constructed out of the same metal as the tank wall, allowing for a very simple and lightweight design. Vanes closely follow the contours of the tank walls. In low gravity, liquid naturally sticks to the vanes and walls in the absence of accelerations. The liquid propellant wets the plate surfaces, and surface tension causes the liquid to form fillets in the corners, thus enabling liquid to be transported along the fillet toward the outlet. Capillary forces then push liquid from one end of the vane to the other near the poles of the tank. Because vanes are open PMDs, they cannot block gas ingestion into the outlet. As propellant is removed via the tank outlet, the weak capillary pumping force can only replace liquid over the tank outlet. This renders stand-alone vanes useless except for liquid resupply in very low acceleration environments with high surface tension propellants, since they are incapable of controlling or holding liquid over the tank outlet. To circumvent this problem, vanes are often used in conjunction with control devices mounted over the tank outlet to provide a very robust PMD.

Table 1 lists the surface tension values of water and several propellants taken from [3]. Vanes and screen channel LADs have been used extensively with storable propellant (propellants that exist as liquids at room temperature) systems using liquids in the intermediate surface tension range, such as nitrogen tetraoxide (NTO) and mono-methyl hydrazine (MMH). However, there is currently no flight operational heritage with cryogenic liquid methane (LCH_4), liquid oxygen (LOX), or liquid hydrogen (LH_2). It is well known that the performance of chemical propulsion systems using cryogenic propellants is approximately equal to (LOX/LCH_4) or much higher (LOX/LH_2) than the storable propellant counterparts. However, the nominal surface tension values are low for cryogens, and given that surface tension is generally a strong function of temperature, it is difficult to design cryogenic PMDs. Furthermore, additional heat and mass transfer effects such as boiling at the wall, evaporation, and condensation all add complexity in design relative to storable propellant PMD design. The focus of this paper is on one technique that may enhance the performance of PMDs.

Fluid	**σ [mN/m]**
Water	65.6
NTO	26.8
MMH	34.1
Methane	13.3
Oxygen	13.2
Nitrogen	8.9
Hydrogen	1.9

Table 1 – Surface Tension Values of Various Fluids

C. Mission Applications

There are two primary space applications where PMDs are or will be employed, in-space cryogenic engines and cryogenic propellant depots. PMDs may be required for Earth-departure cryogenic stages where the engine is restarted in microgravity. PMDs may be required for docking operations between a chemical stage and a propellant depot, or between a chemical stage and a habitat. PMDs are required for ascent and descent stages to and from the surface of the Moon and Mars. PMDs are also required to perform station-keeping maneuvers in microgravity. Finally, PMDs are needed for reaction control maneuvering to return to Earth-orbits. The most recent example of where cryogenic PMDs will be required is in the nuclear thermal propulsion vehicle discussed recently in [6]. Here, each of the drop tanks are depleted in succession; as the tanks drain, liquid flows from the drop tanks to the inline and core tanks, and it will be required to minimize the residuals in those drop tanks (and thus minimize the total required launch mass) before jettisoning them.

Meanwhile for the fuel depot (defined as an Earth-orbiting propellant storage vessel that can house propellant for an indefinite duration of time and then transfer the propellant to any other orbiting vehicle), PMDs may be required to minimize the residuals between the depot storage tank and the customer receiver tank. This is especially true for the case where multiple transfers may be required. Proposed depots could potentially house storable or cryogenic propellants, but the advantage of storing cryogenic fuels is a significant boost in spacecraft performance. Depots will remain in the microgravity of low earth orbit (LEO) for a period of several months up to an indefinite time. Therefore, PMDs will be required to control and maintain liquid flow out of the depot storage tank. The customer vehicle tanks will require very high final liquid volume fill fractions, necessitating the need for robust PMDs upstream in the storage tank. While depot flow rate demands are likely smaller than in-space engine demands, depots may not have the ability to settle liquid over the tank outlet before propellant transfer in the same way that most engines operate; the need for unsettled vapor free, low surface tension cryogenic propellant in the microgravity of LEO makes PMDs an excellent candidate to meet this requirement.

D. Overview of Paper

Given the limiting performance of cryogenic PMDs due to the low surface tension of the cryogenic fluids, the purpose of this paper is to investigate the effects of the femtosecond laser surface processing (FLSP) technique on the performance of a vane-type PMD. The outline of the paper is as follows: First is a high-level background section on the FLSP method and creating omniphilic surfaces. Next, in the experimental hardware section, two different hardware configurations are discussed: the FLSP manufacturing process and the parabolic flight test experiment. Then, experimental results section for FLSP and the flight data from the FLSP-treated guide vane are presented. Finally, the conclusions and future work are discussed.

II. Background

It is well-known that cryogenic PMDs are subject to potentially low performance relative to storable (non-cryogenic) PMDs due to low surface tension and added deleterious heat and mass transfer issues. If a PMD can be made even more "attractive" to a propellant (i.e., omniphilic), then it should perform its function more effectively. One possible way to increase the attractiveness of a PMD is through a laser technology called femtosecond laser surface processing (FLSP) that can be used to change the wetting properties of a surface by creating self-organized, quasiperiodic micro and nanoscale surface features composed of the native target material. It has been demonstrated that FLSP is capable of making metals (and some non-metals) superhydrophilic or superhydrophobic [7-11], and it has the potential to make surfaces omniphilic or omniphobic. FLSP has many advantages over traditional surface functionalization techniques, such as paints, coatings, or complicated nanofabrication methods, including: the production of a fully functionalized surface in a single scalable processing step; the creation of highly permanent hierarchical micro- and nano-scale surface features composed of the original material; the modification of the original surface without mass addition; and the non-reliance on the use of toxic chemicals. By controlling the applied laser parameters, the resulting micro and nanoscale surface features can be tailored to control and optimize either hydrophilic or hydrophobic properties.

Superhydrophilic properties can be achieved by minimal surface preparation and subsequent FLSP treatment. Superhydrophobic results require depositing a low surface energy material onto the surface after FLSP. Only the hydrophilic FLSP treatments will be considered in this paper. Both storable and cryogenic liquid propulsion systems can benefit from enhanced PMDs that are treated to be more omniphilic. The surface tension properties of each cryogen will influence the effectiveness of the PMD and omniphilic FLSP treatment. From Table 1, the performance of the omniphilic FLSP treatment should be comparable for LOX and LCH_4 to what it is for LN_2. LH_2 has very low surface tension, making FLSP likely much less effective with LH_2 than with other propellants. However, the FLSP treatment will likely be very effective with storable propellants, like hydrazine. The eventual goal for this technology is to have a cryogenic storage tank that will have not only omniphilic PMDs, but also tank walls that are omniphobic causing or encouraging the propellant to prefer resting on the PMDs and not the tank wall.

In addition to the flight test and data collection, ground testing of FLSP-treated materials is being performed in Fall of 2022 at Marshall Space Flight Center (MSFC) but is incomplete at the time of this publication. The ground test is measuring the effectiveness of FLSP applied to three materials, titanium, aluminum, and stainless steel 304. The University of Nebraska-Lincoln supplied coupons of each material that were treated to be superhydrophilic that are to be tested for "philic" properties with respect to LN_2. Small sections of FLSP-treated guide vane material were also sent to MSFC. The coupons and guide vane samples are being tested by measuring the contact angle. The ground testing is being performed in a specially constructed vacuum chamber that allows the coupons to be chilled at or below the vaporization temperature of LN_2, thus allowing the measurements to be collected without the complications of mixed phases of LN_2 on the coupon surface. LN_2 is the cryogenic liquid used in all of the testing during this phase of development due to the close match of physical properties of LOX. LN_2 is a much safer cryogen for testing than the actual propellants near this vaporization temperature: LOX andLCH_4. Given surface tension values from Table 1, the performance of the omniphilic FLSP treatment should be comparable for LOX and LCH_4 to what it is for LN_2. $LH_2$is another common propellant, but has very low surface tension making FLSP likely much less effective than it is for other propellants.

III. Experimental Hardware

There are two sets of hardware that were required for this experiment. The first hardware setup was designed and created by the University of Nebraska – Lincoln for FLSP surface functionalization. The manufacturing process for FLSP is still very much in the experimental state. The second hardware setup for the parabolic flight experiment created by Creare is provided.

A. FLSP Hardware – University of Nebraska - Lincoln

The process for manufacturing an FLSP surface is described in this section. A schematic of the experimental setup used to apply FLSP is shown in Figure 5(a). The power incident on the sample surface is controlled via a half-waveplate and polarizer combination. The laser used is a Ti:sapphire based femtosecond (fs) laser (Coherent Astrella) that produces 35 fs, 6 mJ pulses with a central wavelength of 800 nm, at a repetition rate of 1 kHz. FLSP was applied with two different sample translation computer numerical control (CNC) systems. The initial processing was completed on test samples using a 3-axis stage system controlled by LabVIEW code written in-house. The final full-length guide vanes were processed using a CNC system manufactured by 6D Laser that includes a 5-axis sample translation system combined with a galvoscanner that moves the laser beam. The 6D Laser system is controlled using a proprietary fork of SPiiPlusSPC software. The spot size of the laser is controlled by adjusting the distance between the focusing lens and the sample surface with control of the z stage. On the 3-axis CNC system, the pulses are focused using a 150 mm focal length fused silica plano-convex lens. On the 6D Laser CNC system, the pulses are focused using a 163 mm focal length f-theta lens. By raster scanning across the sample, large areas can be functionalized with FLSP. A typical raster scan pattern is shown in Figure 5(b). The laser has a Gaussian spatial profile. The fluence values stated in this paper are peak fluence values calculated for the center of the Gaussian. The pulse count values are calculated based on raster scanning a circle with radius equal to the measured $1/e^2$ laser spot radius. The laser spot size was measured by placing the image plane of a beam profiler at the same z location as the sample surface.

In the work presented here, the peak fluence and pulse count were 1.86 J/cm^2, and 654, respectively. The linear stages have a maximum travel of 400 mm. In order to process the entire 463.6 mm length of the full-length LAD vanes, the galvoscanner was used in combination with the linear stages, which provided an extra 100 mm for processing. However, there were issues with synchronization of the galvoscanner to the stages that led to some non-uniform processing discussed in the experimental results section. Each vane was laser cut to its final dimensions using the same setup after FLSP was applied.

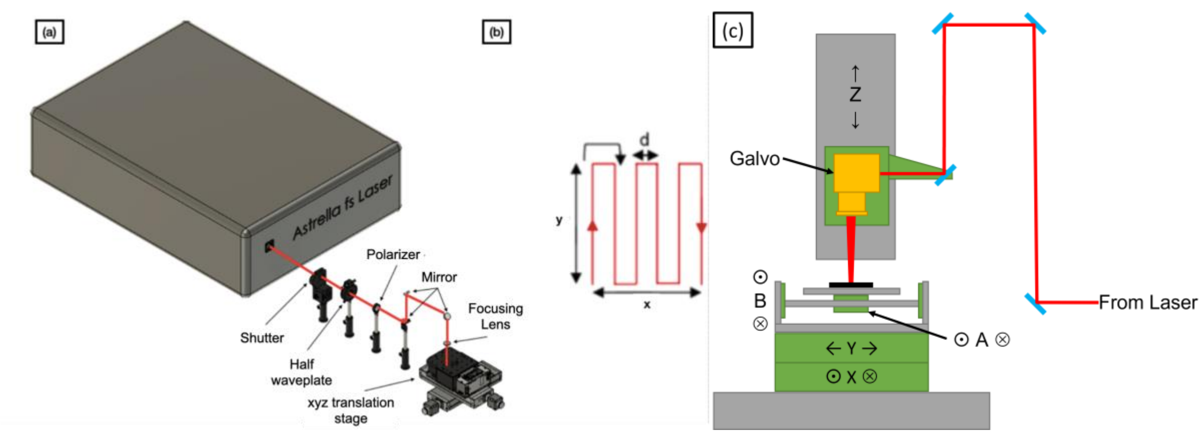

Figure 5 – (a) FLSP Experimental Setup, (b) Standard Raster Scanning Path, and (c) 5-axis CNC Setup with Galvoscanner

After performing FLSP on the materials, the samples were imaged via a scanning electron microscope (SEM) and a laser scanning confocal microscope (LSCM). An FEI Quanta 200 Environmental SEM was used for the SEM imaging and a Keyence VK-X200 LSCM was used to obtain 3D surface profiles and surface roughness information. The full-length guide vanes could not fit in the SEM, so an extra guide vane was processed and cut into small pieces for imaging in the SEM. The LSCM was used to image both the small samples that were imaged in the SEM and the full-length guide vanes and was used as verification of the FLSP structures created on the final guide vanes. After applying FLSP, the wetting properties with respect to water were tested by dropping an approximately 10 mL droplet on the processed LAD samples. The FLSP-processed LAD surfaces were superhydrophilic with zero contact angle and the water droplets wicked completely into the surfaces. Typical contact angles for water and stainless steel surfaces are between 40-70 degrees, so this represents a substantial change in wettability.

Initial trials at applying FLSP to guide vane material, which was 5 mil thick SS304, resulted in issues with warping and therefore non-uniform processing. Different techniques were studied to minimize warping. For the final guide vanes, 10 mil SS304 was used with a mount designed to apply tension to the material during processing. Some work was also completed to investigate "handling" of the FLSP-functionalized guide vane material. FLSP was applied to flat guide vanes and the vanes were bent (rolled) into the final shape needed for the LAD after FLSP. No changes in surface wettability were observed with the handling and bending of the FLSP-functionalized guide vane material.

B. Parabolic Rig – Creare

Creare has developed a hybrid liquid acquisition device (LAD) that synergistically combines screen channel flow structures and lightweight guide vanes [2]. The hybrid capillary structure positions the residual liquid in the tank to optimum locations to maintain liquid supply for LAD screen surfaces, and thus enhances achievable expulsion efficiency. Use of screened channels greatly improves resistance to vapor ingestion in dynamic environments. The screened channel LAD and screened sump are assembled by unique fixturing and laser welding processes to reliably maintain the pore structure of the screen near the bonding joints with its support frames. The additional enhancement of FLSP to the original experiment was added later in the project. Thus, it was desired to determine the impact of increasing guide vane efficiency by treating the guide vanes with FSLP, potentially increasing their affinity for residual liquid propellant by making them more omniphilic.

1. Flight LAD Assembly

The completed LAD assembly is shown in Figure 6. It consists of four individual LAD segments arranged to form two LAD arms. The LAD arms are welded to two supports, which keep the assembly centered inside the primary Dewar and prevent contact between the screen and the Dewar wall during installation. Each LAD arm has four pressure taps positioned axially along its length: the pressure tap tubes then run axially to the front of the LAD assembly, where they are coiled to form a strain relief. The coiled pressure tap ports are then connected to a penetration in the side of the primary Dewar. Each LAD arm has its separate LN_2 outlet tube, and the entire assembly also has a gaseous helium tube which supplies the helium pressurant to the primary Dewar. Three camera mounting rods were positioned in the LAD: one in-between the two LAD arms, and one on the outside of each LAD arm. The cameras and laser emitting diode (LED) lights were positioned on each rod, to permit observation on both the inside and outside surfaces of each LAD arm. All wires and tubing were connected to hermetic passthroughs in the primary Dewar.

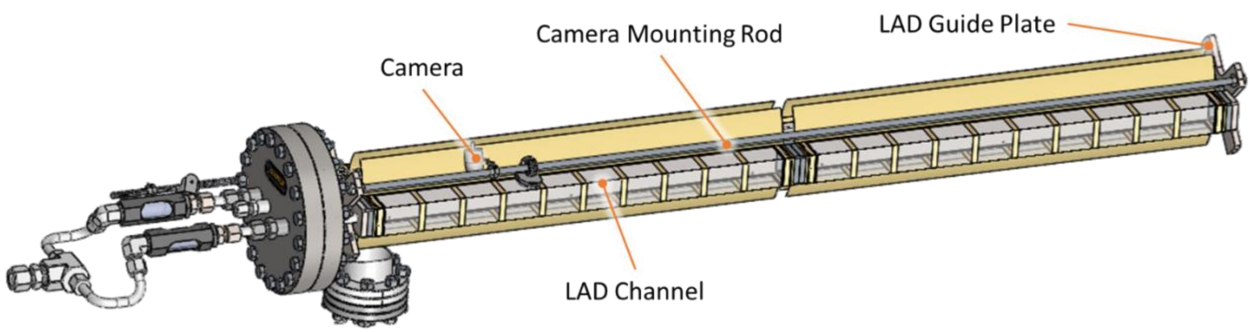

Figure 6 – Completed Fine-Mesh LAD Assembly in Comparison to Solid Model

A closeup view of the front of the LAD assembly showing the coiled pressure tap tubes, tube fittings, and wiring is shown in Figure 7. The pressure measurements were used to determine the pressure drop across the screen during testing and thereby allow calculation of screen permeability. Additionally, the pressure measurements were used to determine the maximum operating pressure drop before vapors broke through the screen and was observed in the outflow. Cameras and LED lights were included inside the primary Dewar LN_2 volume, and also directed at the LAD outflow sight glasses. The cameras inside the Dewar were used to gauge conditions inside the Dewar, including the liquid-vapor distribution and the interaction between the LAD and the liquid. The cameras observing the outflow sight glasses were used to ensure that the LAD was effectively draining only liquid from the Dewar, and would provide direct evidence of the moment that vapors broke through the LAD screen and entered the outflow channel.

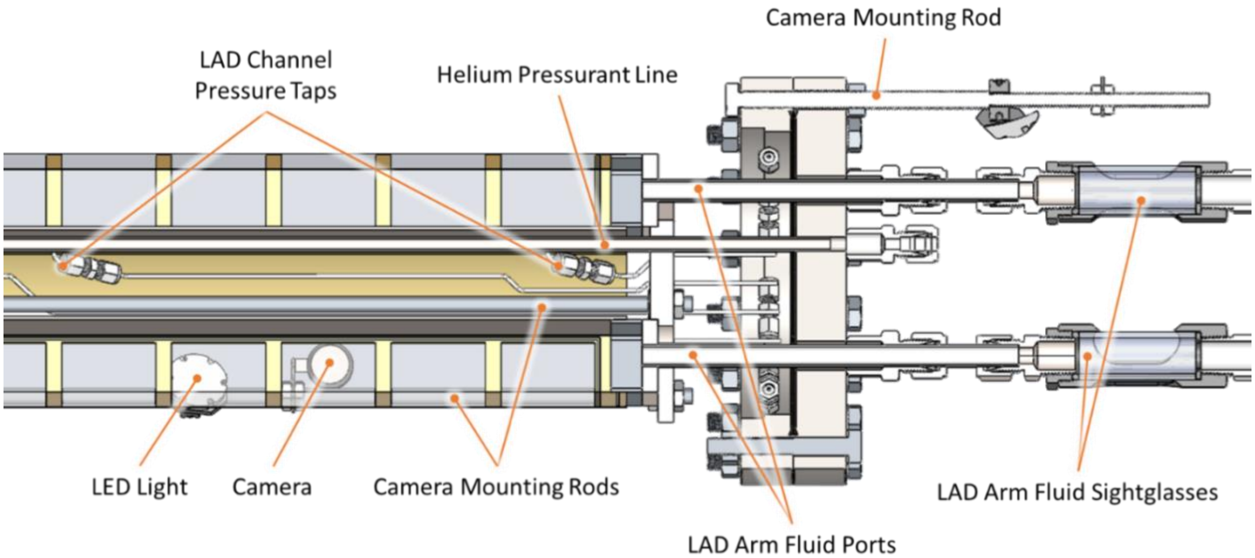

Figure 7 – Closeup View of Front of LAD Assembly in Comparison to Solid Model

The two parallel LAD channels provide an opportunity for evaluation of the FLSP treated guide vanes in direct comparison to untreated guide vanes. As shown in Figure 8, one set of guide vanes was treated with the FLSP technique, while the other set of guide vanes was untreated stainless steel material. Parallel sight-glasses positioned at the outlet of each segment allow this assessment to be made visually.

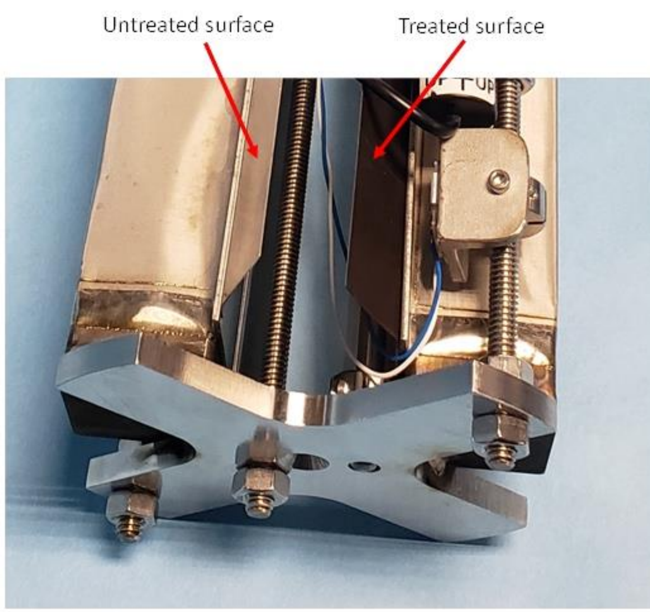

Figure 8 – Photograph of LAD Assembly with Treated and Untreated Surfaces Visible

Before assembling the experiment, checkout testing of the LAD assembly was conducted, including bubble point testing by submerging in isopropyl alcohol and flowing air into the internal volume. While evaluating the LAD in benchtop testing, qualitative observations were made of the guide vanes surfaces under direct contact with LN_2, as shown in Figure 9. In these photographs, LN_2 is poured from a thermos directly onto the LAD guide vanes, in open air—first onto the bare SS surface, then onto the FLSP-treated surface from UNL. After a few seconds, the guide vane was sufficiently chilled down, and wetting behavior on these two surfaces was observed. For the FLSP-treated surface, an enhanced wicking effect was evident that allowed for a wetted spot that was sustained longer in open air. This behavior was consistent with the enhanced wettability desired by the authors for the present application.

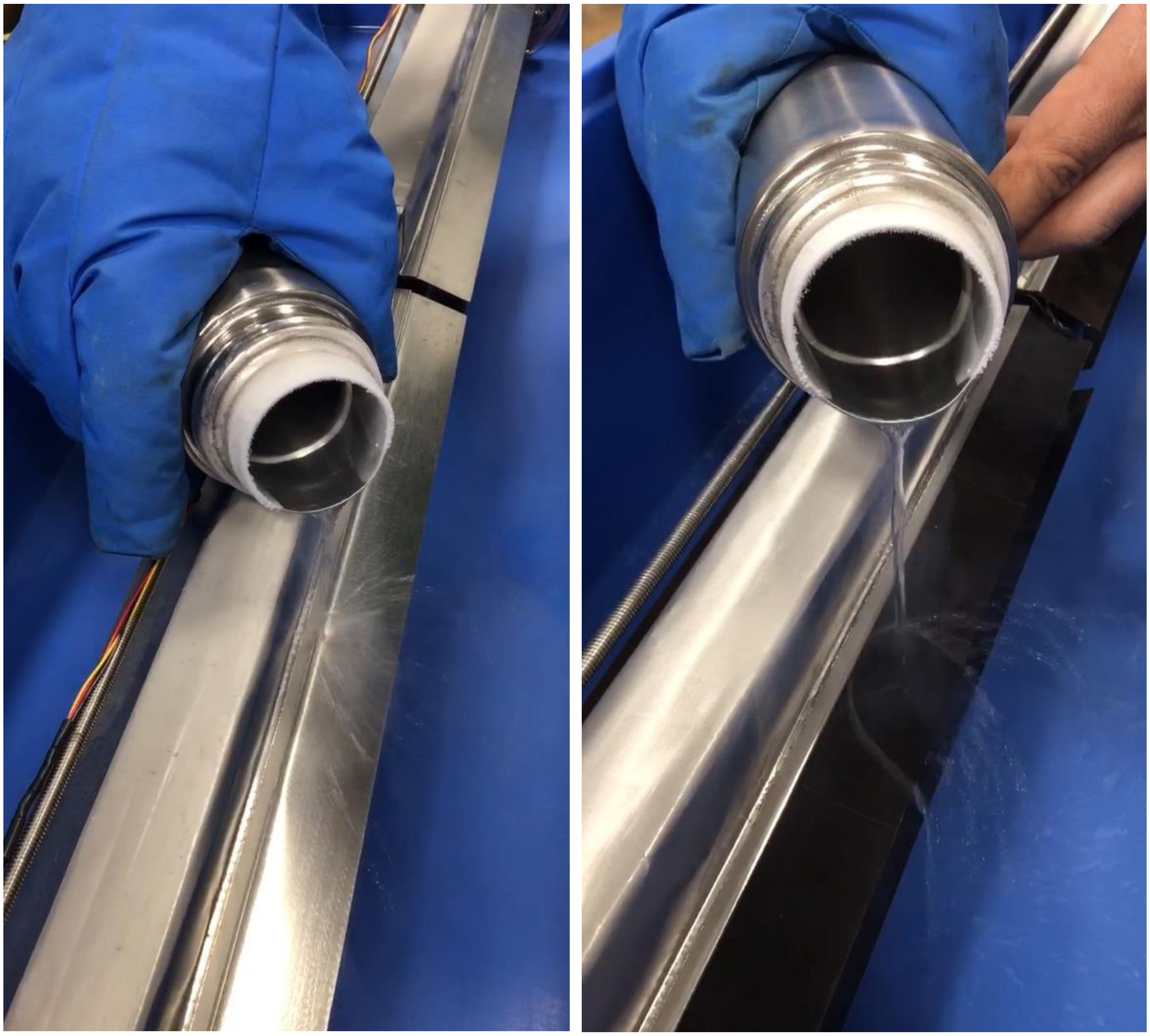

Figure 9– Photograph Showing Wetting Properties of Guide Vane Under LN_2 Contact. (Left) Stainless Steel Guide Vane. (Right) Stainless Steel Guide Vane with FLSP Treatment.

Once characterized in open air testing, the completed flight LAD with guide vanes was then placed within the primary Dewar LN_2 chamber. A conflat flange on the side of the LN_2 chamber Dewar sealed the eight pressure taps, and a conflat flange on the top of the chamber sealed the LN_2 liquid lines, the helium line, and the electronic plugs. The primary Dewar LN_2 chamber was outfitted with low conductivity G10 blocks to provide support both radially and axially when it was placed within the vacuum chamber. The pressure transducers that monitor the LAD assembly were mounted to the exterior of the LN_2 chamber within the vacuum chamber to minimize any parasitic heat loss that could interfere with accurate pressure measurement. Finally, the two liquid outlet lines from the LAD assembly were connected to sight glasses and then merged into one common liquid outlet leg for the primary Dewar. A camera positioned within the vacuum chamber looked at both sight glasses and would be used to determine when bubbles have broken through the screens. The camera and outlet sight-glasses reside in the vacuum space to limit heat leak. Views of the primary Dewar LN_2 volume are shown in Figure 10.

2. *Parabolic Flight Test Rig*

The LAD assembly is housed in the parabolic flight test rig, which consists of a primary (horizontally-inclined) Dewar, a receiver Dewar, a supply Dewar, and a helium gas cylinder, as well as associated valves, plumbing, and support hardware (Figure 11 and Figure 12). All pressure relief valves vented to a heated section and containment tank to prevent any LN_2 from entering the aircraft vent port.

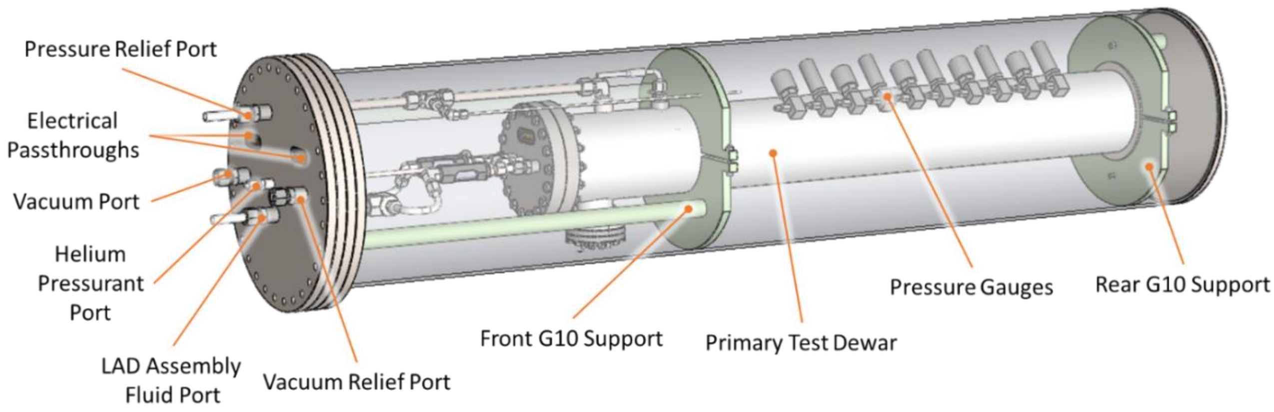

Figure 10 – Primary Dewar: LN_2 Test Section with Internal LAD Assembly, within Vacuum Chamber

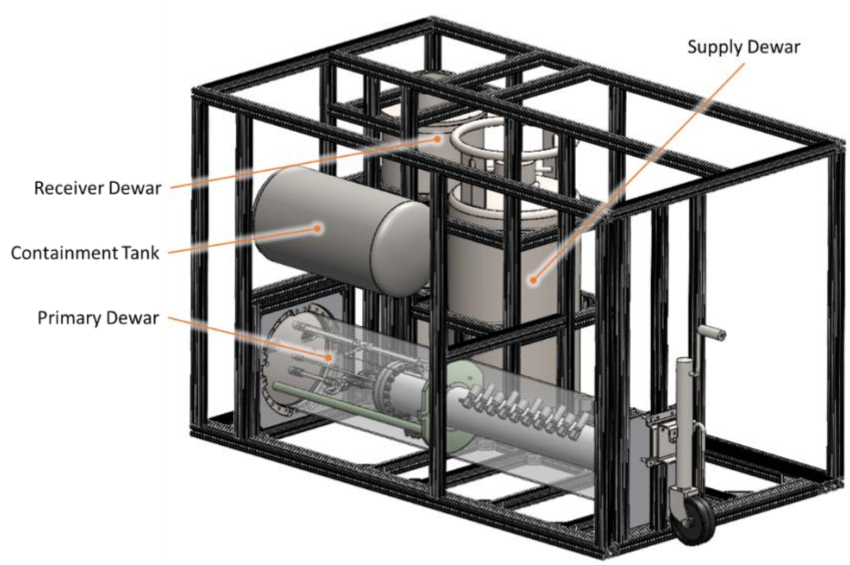

Figure 11– Test Facility Ready for Ground Testing (Pre-Flight)

The concept of operations for the test facility during parabolic flights is as follows. Based on the estimated cycle time to complete a given test, multiple full test cycles could occur during each parabolic flight (up to 30 cycles of 15–20 seconds each), thus the planned test matrix included full draining of the tank via the LAD with several unique flow rates ranging from 50 g/s to 400 g/s. Higher flow rates permitted a larger number of test cycles in a given flight. Data acquired for each test included visual data inside the length of the Dewar to observe the two-phase distribution within the Dewar during outflow, as a function of gravity, and pressure measurements along the length of the LAD during outflow. The point of LAD breakdown was determined by collapse in observed liquid flow as measured by the flowmeter. In post processing, visual indicators clearly pin-pointed the moment of breakdown including camera recordings of the in-line sight-glass.

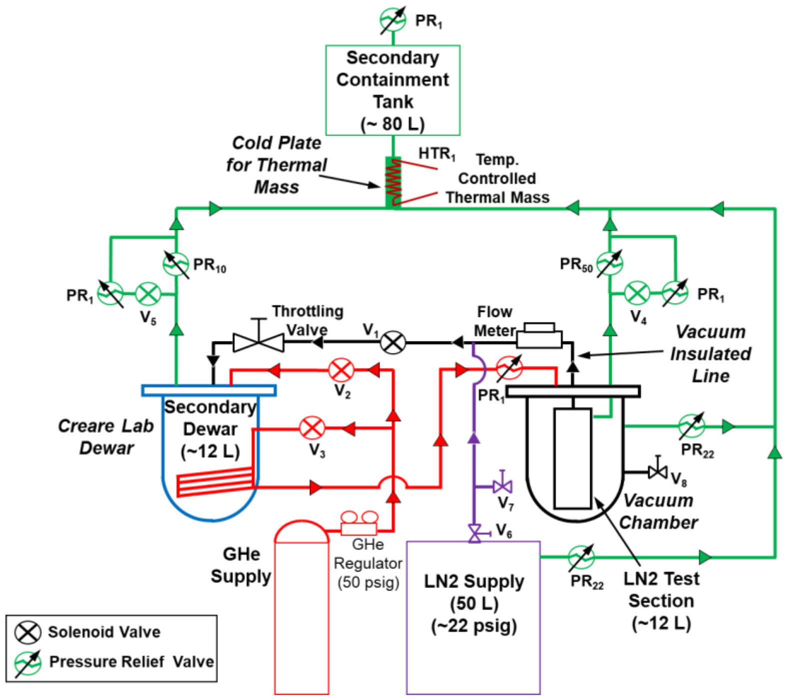

Figure 12– Schematic of Parabolic Flight Test Facility

The flight test rig is designed specifically for the particular flight characteristics of a parabolic flight. Typically, testing of large-scale LADs in a 1g environment is not possible with a screen channel longer than 12″ due to hydrostatic (gravity) forces. This limits the relevance of ground testing for screen channel LADs and many other surface tension devices. In contrast, the present LAD test assembly is positioned within a custom horizontal LN_2 Dewar that is 60″ long, with a maximum diameter of 5″, and lying on the floor of the aircraft. During the parabolic flight, acceleration perpendicular to the axis of the aircraft ranges from near-0g to 2g. However even conditions up to 2g cannot cause vapor to penetrate the screen channel because its length perpendicular to the floor is only 5″. It is feasible to conduct outflow testing in near-zero-g during periods of microgravity, then shut off the demand valve when higher accelerations occur, and the LAD will survive these interim periods of high acceleration. This arrangement enables the LAD assembly to empty a relatively large supply tank over the course of an entire parabolic flight, instead of limiting its use to a brief 15–20 second window with a small test article. Significantly, this enables demonstration of the LAD technology in a size and configuration that would be representative of future commercial and NASA applications.

After finishing assembling the facility, several ground tests were performed to evaluate system performance and verify the ability to control LN_2 transfer during parabolic flights. Specifically, these tests demonstrated that the system functioned as intended and could be operated during the short, ~15 s windows of microgravity expected during parabolic flights. It was also demonstrated that the facility could successfully transfer LN_2 from the receiver Dewar back into the primary Dewar which allowed performing several tests during a single flight cycle. Differential pressure gauges were monitored to determine the breakthrough pressure for the LAD assembly. For these ground tests, breakthrough was demonstrated to occur at the point that the LAD channels became fully uncovered. In microgravity conditions, the two-phase distribution within the tank is expected to be surface tension-dominated, meaning that much more than half of the liquid can be transferred without drying out the LADs.

While the pressurant was being applied to drive LN_2 from one Dewar to the next, helium and vaporized LN_2 was vented through a cryogenic check valve to maintain a given pressure setpoint. In microgravity, this vented gas may contain entrained LN_2 droplets since it will no longer be settled on the bottom of the tank. Thus, a secondary containment was included to collect the vented helium/LN_2 mixture. Resistive heaters boiled off residual LN_2 that entered this containment during the venting process. The contained volume could be vented overboard during all portions of the flight including the microgravity periods, since the gas mixture was sufficiently warmed prior to venting.

IV. Experimental Results

Once again, there are two different hardware setups, each with their own results to be presented. The results of each experiment are presented in the previously established order: FLSP and finally the parabolic flight results.

A. Femtosecond Laser Surface Processing (FLSP) results – University of Nebraska - Lincoln

The LAD design presented in this paper involves guide vanes composed of thin SS304 material. The target thickness was 5 mil, however, because of issues with warping discussed below, 10 mil SS304 was used in the final design. Figure 13 includes SEM images of FLSP microstructures created on a small test sample and these serve as the target structures for the final guide vanes. Figure 13 also includes an LSCM 3D height map of the FLSP structures. The structures had an average height of 27.19 µm with a standard deviation of 3.00 µm.

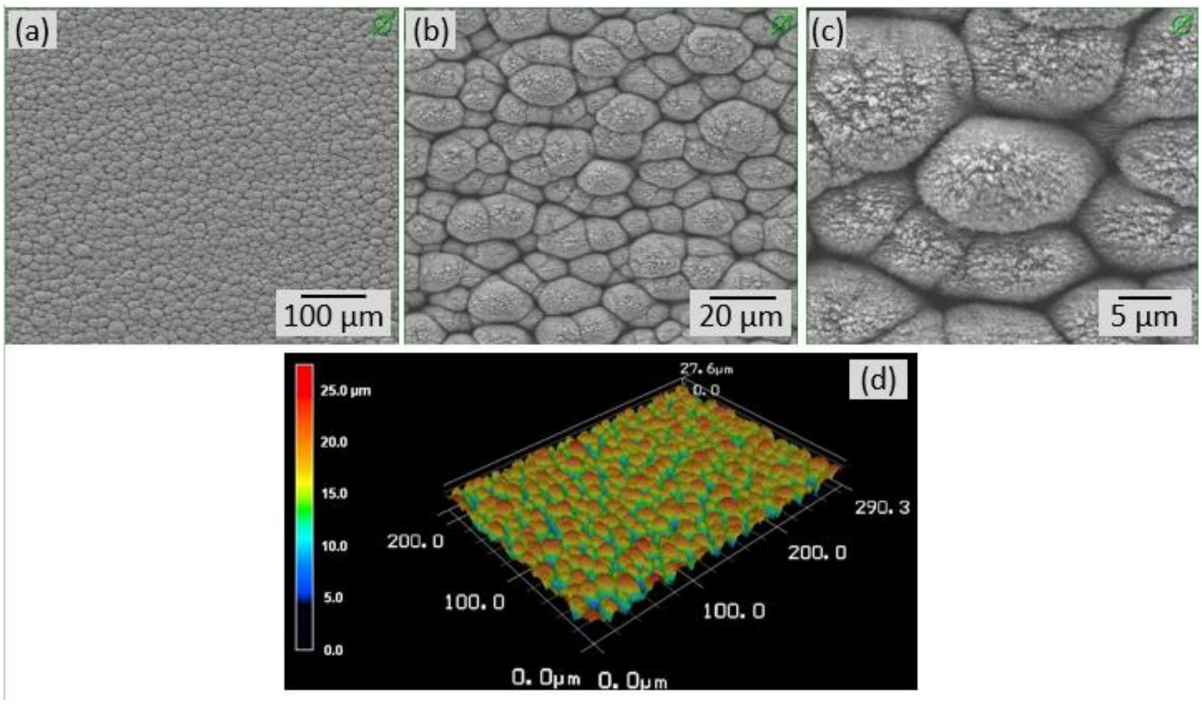

Figure 13 – SEM Images of The FLSP Structures Produced on the LAD Guide Vanes. The Magnification is Increased Moving From (A) to (C). (D) LSCM 3D Height Map of the FLSP Structures Produced on the LAD Guide Vanes

To produce consistent FLSP microstructures across the guide vanes, the samples must remain flat during processing. Furthermore, the guide vanes need to remain reasonably flat for welding them to the LAD structure. Initial work on applying FLSP to 5 mil thick SS304 resulted in warping even with the samples clamped on the ends. For this initial work, 1 in wide x 6 in long SS304 samples were used. The 3-axis homebuilt CNC system was used to apply FLSP. Figure 14 includes pictures of 5 mil thick SS304 guide vane material before and after applying FLSP. The samples were clamped on each end, however, when applying FLSP the samples warped and eventually broke free from the clamps. The final result was a surface with non-uniform FLSP structuring and a warped guide vane. Therefore, work discussed below was completed to develop techniques to apply FLSP to the thin SS304 samples without warping.

A second attempt at applying FLSP without warping included improvements to the clamping as shown in Figure 15. With the improved clamping, the samples remained clamped during the entire FLSP process. While this reduced the warping, there was still some warping of the samples as shown in Figure 16. LSCM images were collected at different locations across this sample, including at different locations along the warped surface and are included in Figure 17. From the LSCM analysis the warping did not have a significant effect on the FLSP surface features.

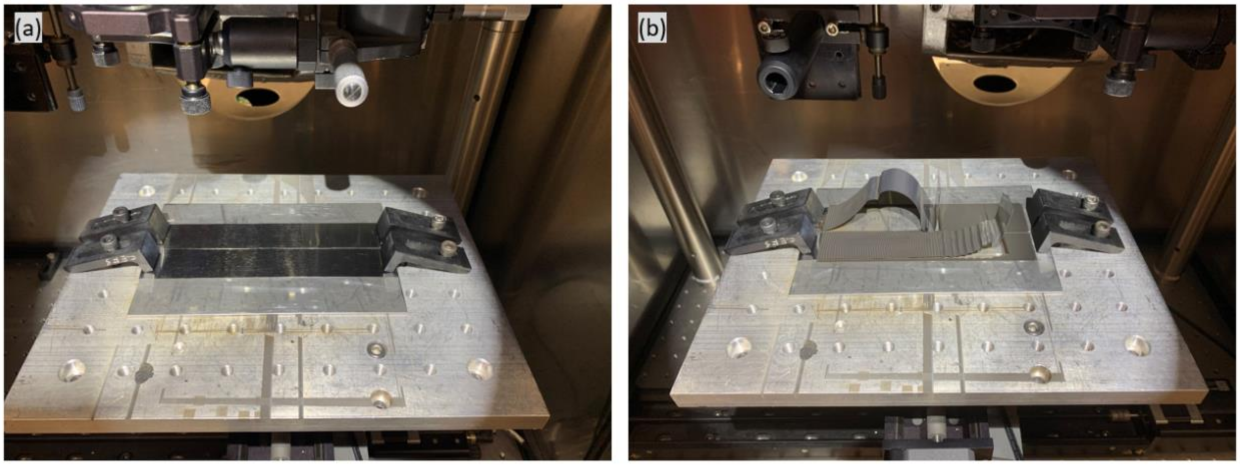

Figure 14 – 5 mil Thick SS304 (a) Before and (b) After Applying FLSP

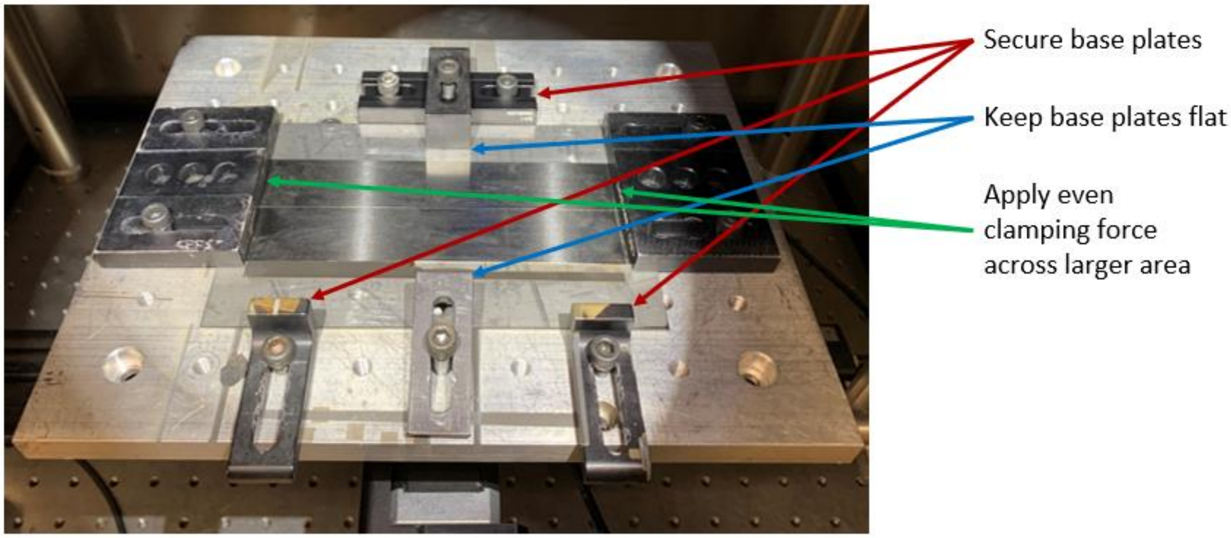

Figure 15 – Improved Clamping of the Guide Vane Test Strips During FLSP

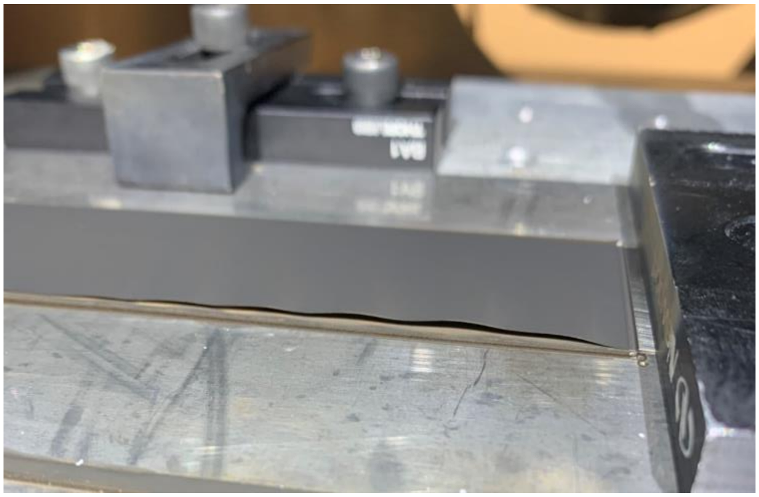

Figure 16 – Guide Vane Test Strip After Applying FLSP with Improved Clamping

In an attempt to prevent warping, 5 mil samples were glued to a thick metal plate using Aremco Crystalbond™ 509 adhesive. When applying FLSP, the laser processing broke the adhesive bond and the samples started to warp in Figure 18(a). A plate was added during processing to hold the sample flat (Figure 18(b)). Some adhesive was melted by the laser and wicked to the laser processed side of the sample, contaminating the sample surface. Not shown in Figure 18, the same process was repeated with mechanical clamping of the samples in addition to the adhesive and gave similar results with warping of the sample and contamination of the laser processed surface with adhesive. Since the samples still warped and became contaminated with the adhesive on the FLSP side, gluing the samples was not pursued further.

While the sample shown in Figure 18 resulted in minimal warping and contained uniform FLSP features, there was a concern that the warping would be exaggerated when extending to the full-length guide vanes. Therefore, for the final LAD samples, a high-tension mount was developed to hold the samples flat (see Figure 19) and 10 mil thick material was used. This resulted in uniform FLSP structures across the entire guide vane without warping of the material. The final full-length guide vanes (34.8 mm wide and 463.6 mm long) were processed on the 6D Laser CNC system. The CNC system included stages with 400 mm of travel and a galvoscanner that moved the laser beam with 100 mm of travel. To process the entire 463.6 mm of the full-length guide vanes, the galvoscanner and stages were both used. The CNC system was programmed to scan a 66.2 mm length section of the guide vane using the galvoscanner. Then the galvoscanner would reset back to the start of the galvoscanner processing area and the stages would move 66.2 mm to enable processing the subsequent 66.2 mm section of the guide vane. There was some error in the stitching that has not yet been resolved and resulted in a lower pulse count at the stitch points, and therefore, slightly smaller FLSP structures that are visible as a slight color change on the final guide vanes as shown in Figure 19. For the starting and ending lengths of the guide vanes, the galvoscanner was programmed to scan a 33.1 mm length, so the first region of the guide vane in Figure 19 before reaching the first stitch is shorter than the subsequent regions. Furthermore, the laser shutter system was too slow to respond at the speed of the galvoscanner, so when the galvoscanner reset back to zero, the sample was hit with a few pulses across the processed area. These resulted in a color change, but little change in the FLSP structures. These areas did not affect the wetting properties of the surface. When a droplet was placed near an ablation crater or a stitch line, the water wicked and uniformly wetted the entire area. Figure Figure 20 includes SEM from a sacrificial full-length guide vane that was cut into small sections for imaging. SEM images of the FLSP features are included for each end of the guide vane as well as a stitch line and an ablation spot from a galvoscanner reset.

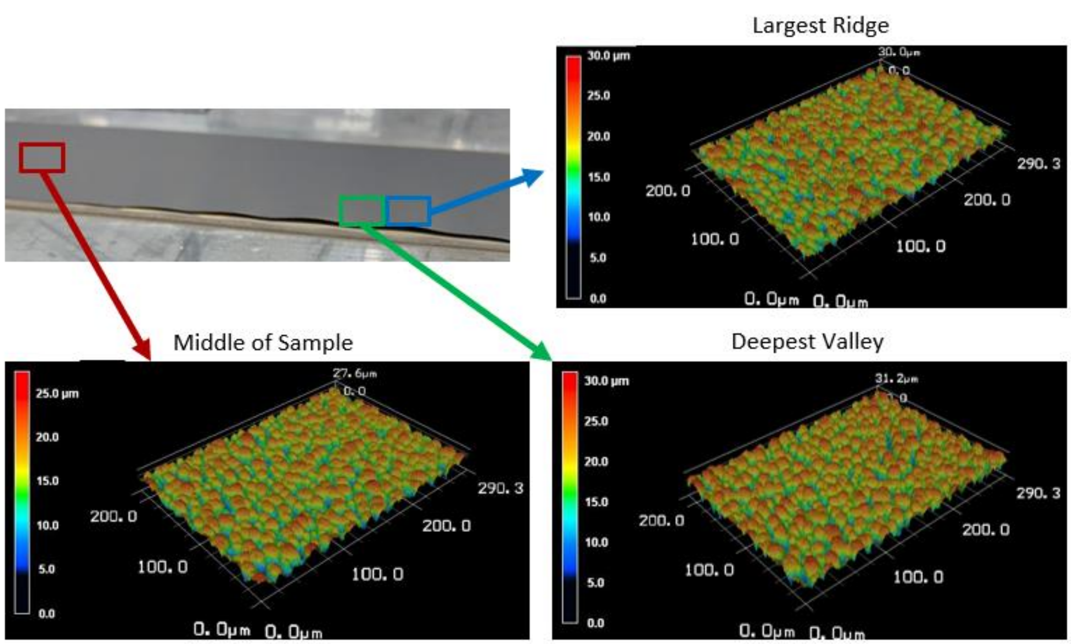

Figure 17– LSCM Height Maps of the FLSP Features at Different Locations on the Warped Guide Vane. (Top-left) Picture of the FLSP-processed Guide Vane with Locations where LSCM Height Maps were Captured Outlined with Boxes

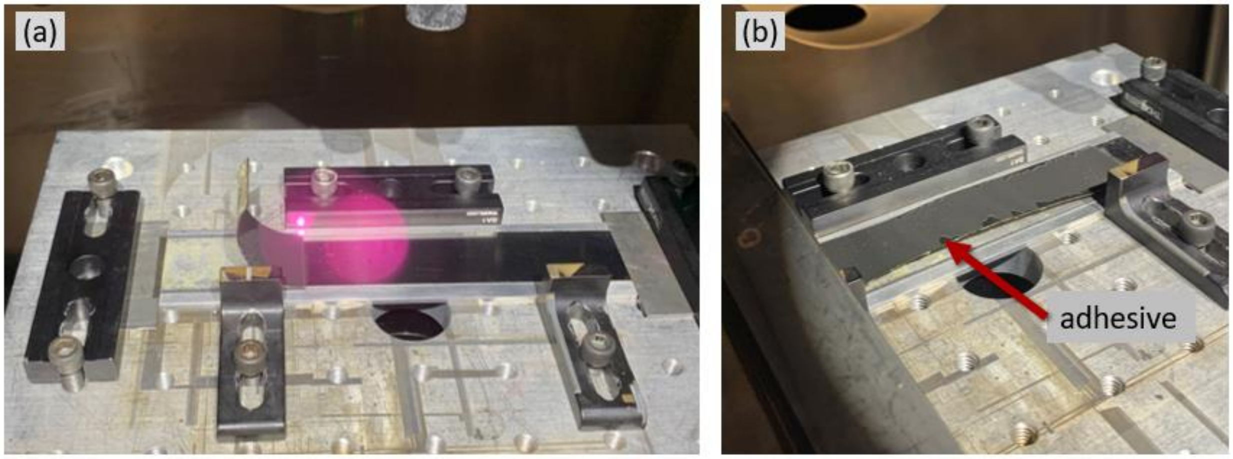

Figure 18 – FLPS Applied to Guide Vane Strips That Were Glued to a Thick Plate and not Clamped on the Ends

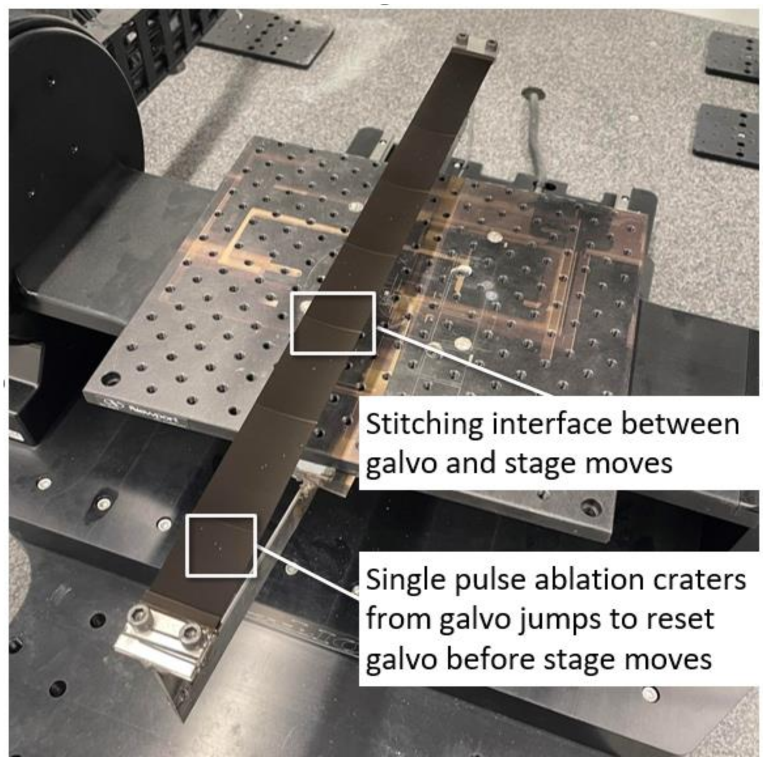

Figure 19 – Full-length Guide Vane after FLSP

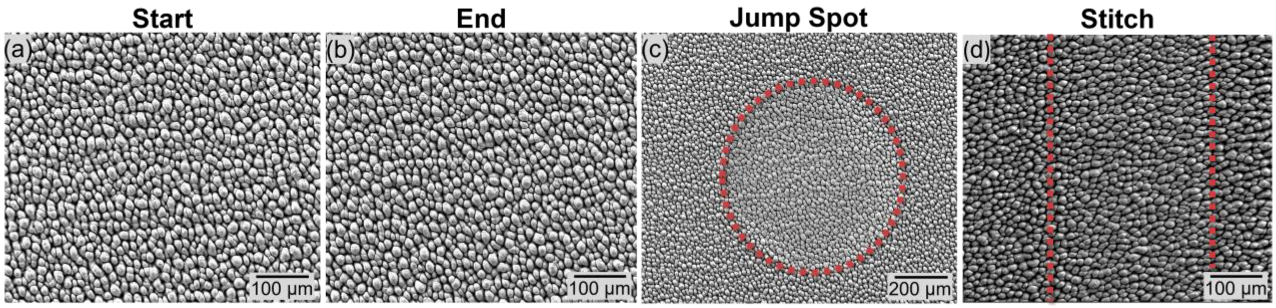

Figure 20 – SEM Images of the FLSP Features on a Full-Length Guide Vane That was Cut into Small Pieces for SEM Imaging

Applying FLSP results in removal of some amount of material from the surface. To quantify this material removal, 5 mil thick guide vane test strips were weighed before and after FLSP. The material removal rate will be the same for the 10 mil thick material as the 5 mil thick material. The material removal rate was calculated as the start mass minus the end mass divided by the area. Table 2 includes the mass before and after processing and the calculated material removal rate.

Sample	Start Mass (g)	End Mass (g)	Area (mm^2)	MRR (g/m^2)
T3 (1 in x 6 in SS304 strip, 5 mil thick)	7.5201	7.2651	3402	74.9559
T4 (1 in x 6 in SS304 strip, 5 mil thick)	7.4688	7.2193	3402	73.3392

Table 2 – Mass of 1 in x 6 in SS304 Strips Before and After Applying FLSP to One Side and the Material Removal Rate.

B. Parabolic Flight Experimental Results

Over the course of the parabolic flight test campaign, the LAD assembly was demonstrated to successfully transfer vapor-free cryogenic LN_2 at several stable flow rates corresponding to the prescribed test matrix, and key performance data was generated to establish performance of this technology in microgravity. Measurements indicated that at conditions of observed LAD breakdown, the supply tank housing the hybrid LAD contained less than 5% of its initial LN_2 fill, for a tank expulsion efficiency of at least 95%. This result is highly encouraging for the technology overall and is in line for performance targets for future mission needs. These results are being summarized for a companion paper describing general characteristics of the LAD performance in microgravity.

For the present investigation into impact of FLSP-treated guide vanes, the intent was to closely examine the liquid/vapor distribution along the guide vanes using internal video cameras, including looking for differences on the guide vane with cryophilic (omniphilic) treatment. A photograph of the LAD test assembly partially wetted by LN_2 during microgravity LN_2 flow is shown in Figure 21. In this view, the guide vane appears to assist in capturing LN_2 in the vicinity of the screen channel to facilitate enhanced expulsion efficiency. While videos of microgravity liquid transfer were captured between the internal cameras, and several breakdown events recorded, it was difficult to obtain more quantitative differences between the LAD channels in low-g. Videos from inside the tank during the parabolic flight tests also revealed that the tank liquid/vapor distribution is relatively dynamic, especially in portions of testing when a reasonably high fraction of liquid remains in the tank. The ideal condition for observation of the guide vane behavior, in particular impact of the FLSP-treated surfaces, would be a quiescent liquid distribution dominated by surface tension forces. One way to achieve this configuration might be to reorient the test rig by rotating 90 degrees such that the long axis is parallel to the long axis of the aircraft.

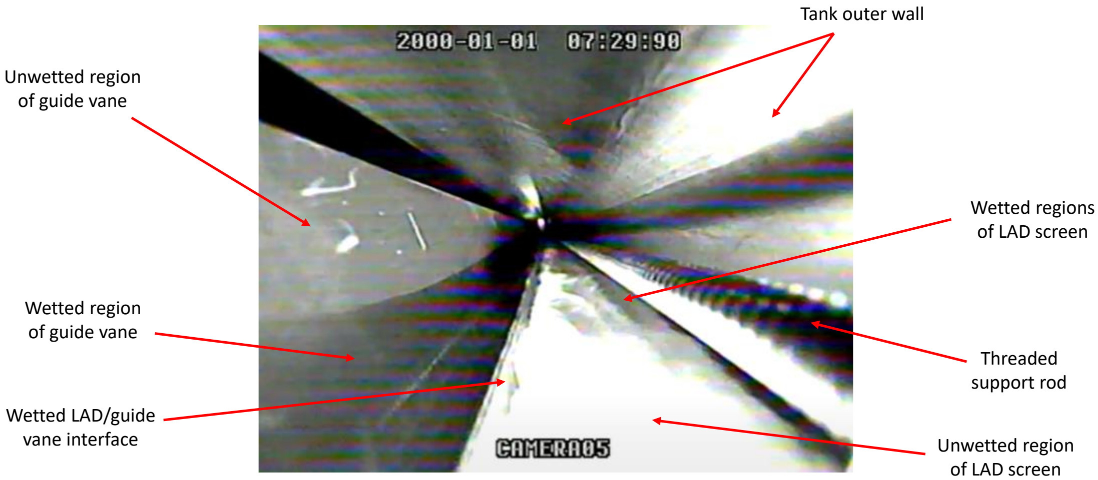

Figure 21 – View of LAD Test Article with FLSP-treated Guide Vane During Microgravity Testing; Guide Vane Appears to Assist Wetting of Partially-covered Screen Channel Surface

V. Conclusion

In this paper, femtosecond laser surface processing (FLSP) was investigated as a surface functionalization technology to enhance cryogenic liquid acquisition devices (LADs) and was shown to be successful. In summary:

1. The FLSP process was successfully carried out on subscale stainless steel guide vanes.
   The target was 5 mil thick stainless steel, however, due to issues with warping, the final guide vanes were 10 mil thick. With further work on optimizing FLSP parameters and the sample mounting techniques for applying FLSP, it may be possible to apply FLSP to 5 mil thick stainless steel guide vanes without warping to reduce the mass of the guide vanes. It should also be considered that FLSP results in some mass loss that was measured to be about 74.1 g/m^2 of processed area for the parameters used for processing the guide vanes.

2. It was demonstrated that FLSP can be applied to full size LAD guide vanes (34.8 mm wide by 463.6 mm long) composed of 10 mil thick stainless steel without warping the material. Furthermore, it was also demonstrated that full size guide vanes can be processed with FLSP to create a superhydrophilic/supercryophilic surface, bent into the final form, and welded to the LAD structure without damaging the FLSP surface.

3. Ground testing conclusively showed an improved contact angle with a water contact angle of zero and improved wettability on the treated guide vanes compared to a smooth stainless steel surface when LN_2 was poured onto the surfaces in ambient conditions.

4. FLSP-treated guide vanes were successfully incorporated into a test rig for reduced gravity cryogenic testing.

5. Flow visualization shows that the guide vane appears to assist in capturing LN_2 in the vicinity of the screen channel to facilitate enhanced expulsion efficiency.

Follow-on flight testing is desired to better orient the payload to allow for a more quiescent environment. Meanwhile, UNL continues the development of FLSP to experiment with the opposite effect, omniphobic surface treatment. The intended goal for cryogenic propellants could be to treat the tank walls such that they would more easily liberate liquid from the tank walls, making it more likely to migrate to the LADs. UNL continues to work with NASA to test a variety of coupons.

Acknowledgments

This work was partially supported by NASA SBIR Phase IIE and by NASA Nebraska Established Program to Stimulate Competitive Research (EPSCoR.)

References

[1] Hartwig, J.W. "Propellant Management Devices for Low Gravity Fluid Management: Past, Present, and Future Applications" *AIAA Journal of Spacecraft and Rockets* Vol. 54, No. 4, 808 – 824. 2017.

[2] Conboy, T.M., Daines, G.W., O'Neill, L., Zagarola, M., and Hartwig, J.W. "Development of a Hybrid Screened Channel Liquid Acquisition Device for Reliable Microgravity Transfer of Cryogenic Fluids" *Cryogenics* 2022.

[3] Hartwig, J.W. "Liquid Acquisition Devices for Advanced In-Space Cryogenic Propulsion Systems", Elsevier: Boston, MA, November, 2015.

[4] Jaekle, D.E. "Propellant Management Device Conceptual Design and Analysis: Vanes" AIAA-91-2172, 27th Joint Propulsion Conference, Sacramento, CA, June 24 – 26, 1991.

[5] Tegart, J.R. "A Vane Type Propellant Management Device" AIAA-97-3028, 33rd Joint Propulsion Conference, Seattle, WA, July 6 – 9, 1997.

[6] Meyer, M., Hartwig, J.W., Sutherlin, S., and Colozza, A. "Recent Concept Study for Cryogenic Fluid Management to Support Opposition Class Crewed Missions to Mars" *Cryogenics* 2023.

[7] Kruse, C. *et al.* Effects of Femtosecond Laser Surface Processed Nanoparticle Layers on Pool Boiling Heat Transfer Performance. *Journal of Thermal Science and Engineering Applications* **10**, 031009 (2018).

[8] Vorobyev, A. Y. & Guo, C. Metal pumps liquid uphill. *Applied Physics Letters* **94**, 224102 (2009).

[9] Huang, C., Bell, R., Tsubaki, A., Zuhlke, C. A. & Alexander, D. R. Condensation and subsequent freezing delays as a result of using femtosecond laser functionalized surfaces. *J Laser Appl* **30**, 011501 (2018).

[10] Zuhlke, C. A. *et al.* Superhydrophobic metallic surfaces functionalized via femtosecond laser surface processing for long term air film retention when submerged in liquid. in *Proc. SPIE* (eds. Klotzbach, U., Washio, K. & Arnold, C. B.) vol. 9351 93510J (2015).

[11] Vorobyev, A. Y. & Guo, C. Direct femtosecond laser surface nano/microstructuring and its applications. *Laser Photon Rev* **7**, 385–407 (2013)